High-order QAM 10-GHz-class Intermediate-Frequency-over-Fibre Transmission with Digital Pre-emphasis and an FPGA-based Receiver

Junya Nishioka, Takatoshi Akamatsu, Michiya Hayama, Keita Mochizuki, Tsuyoshi Yoshida, and Naoki Suzuki

IT R&D Center, Mitsubishi Electric Corporation, Nishioka.Junya@aj.MitsubishiElectric.co.jp

Abstract *We evaluated a transmission system with 28 Gsps digital-down-conversion and pre-emphasised intermediate-frequency-over-fibre. The system accommodated four OFDM-16QAM signals of 1.5 GHz bandwidth. For OFDM-64QAM, the EVM was only 0.6% short. An ADC which has an ENOB of 6 enables the system to transmit OFDM-64QAM.*

Introduction

In recent years, discussion of beyond-fifth generation (beyond-5G) mobile access systems has been quickening for radio access networks (RAN). Beyond-5G systems will provide advanced broadband service with 10 times greater performance than 5G systems [1]. Beyond-5G, mobile access systems need higher frequency radio signals to yield bandwidth of up to several GHz, more than current systems [2].

In general RAN architectures for 5G or after, a distributed unit (DU) controlling the radio communication, and radio units (RUs) incorporating the radio transceivers are connected over mobile fronthaul (MFH) systems. The connections use on-off keying (OOK) digital optical transmission with the common public radio interface (CPRI) formats [3–5]. CPRI requires about 16 times greater bandwidth than the radio signals due to the data waveform using OOK. Hence it is difficult to transmit several GHz signals by simply using the existing formats. To overcome this problem, the radio-over-fibre technique (RoF) offers a breakthrough. RoF technology can deliver high carrier frequency, ultra-broadband radio signals such as millimetre-wave with over 1 GHz bandwidth by using analogue optical transmission [6–8]. As an advanced RoF technology, the intermediate-frequency-over-fibre (IFoF) technique has been investigated. An IFoF-based MFH can efficiently carry multiple radio frequency signals aggregated onto intermediate frequencies (IFs) by using analogue optical transmission with a wide bandwidth such as 10 GHz [9–13].

An IFoF receiver must demultiplex the IFs. Digital demultiplexing has been investigated as a good approach that has the advantages of small circuit size, steep filter cut-off and design flexibility [9–13]. We have investigated a wideband, high throughput demultiplexer using multi-stage digital-down-conversion (DDC) with a 28 Gsps analogue to digital converter (ADC) for beyond-5G. However, demultiplexers have yet to demultiplex IF channels with offsets of ≥10 GHz. This is due to an inadequate signal-to-noise-ratio (SNR) because of an insufficient effective number of bits (ENOB), and the frequency responses of the electrical and optical devices including the ADC, optical modulator and photo diode (PD) [14]. To overcome this, pre-emphasised IFoF (PEIFoF) is effective [4,13].

In this paper, we report a wideband PEIFoF generation scheme with a digital demultiplexer and demonstrate PEIFoF transmission carrying four aggregated IF channels. In this demonstration, we evaluated the performance of IF channel demultiplexing with an IFoF receiver prototype equipped with a 28 Gsps ADC and a 3-stage DDC implemented in a field programmable gate array (FPGA) as a low latency real-time processor.

Experimental setup and PEIFoF Calibration

In this section, the details of the IF channel demultiplexing are explained. Fig. 1 shows the experimental setup for evaluating the PEIFoF transmission system from DU to RU with a DDC demultiplexer. At the DU side, the PEIFoF signal was generated by a 56 Gsps arbitrary waveform generator (AWG). The PEIFoF signal waveform data was calculated by offline signal processing of the four wideband IF waveforms. These were orthogonal frequency division multiplexing (OFDM) signals of 1.5 GHz bandwidth and were modulated by 16-ary or 64-ary quadrature amplitude modulation (16QAM/64QAM) with IF offsets of 2.25 GHz, 5.25 GHz, 8.25 GHz and 11.25 GHz, which we call channels #1–4 (chs #1–4). They had 320 data subcarriers spaced at 3.9 MHz, and 63 pilot subcarriers (interval: 6), which was required to correct any phase and amplitude fluctuations due to transmission gain, frequency shifter phase, and so on. Then the

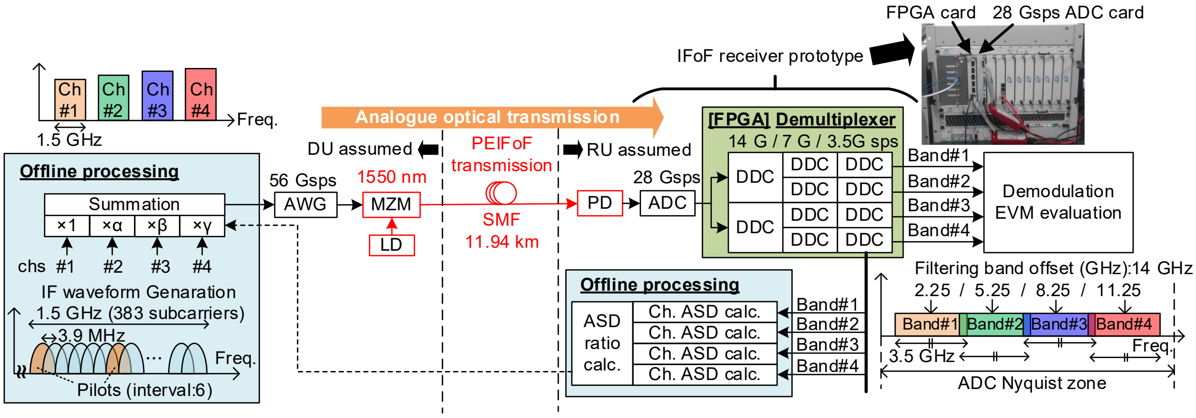

Fig. 1: Experimental setup to evaluate the PEIFoF transmission system with DDC demultiplexer.

Tab. 1: Latency of DDC processing.

Function name		Number of clocks	Clock rate	Latency
1st stage DDC	Frequency shift	8 clocks	312.5 MHz	25.6 ns
	HBF and 1/2 decimation	11 clocks		35.2 ns
2nd stage DDC	Frequency shift	8 clocks		25.6 ns
	HBF and 1/2 decimation	11 clocks		35.2 ns
3rd stage DDC	Frequency shift	8 clocks		25.6 ns
	HBF and 1/2 decimation	11 clocks		35.2 ns
Total latency of DDC processing				**182.4 ns**

waveforms of chs #1–4 were multiplied by pre-emphasis factors 1, α, β and γ. The four chs #1–4 were multiplexed onto the PEIFoF signal by summation. The PEIFoF signal generation was realized easily by amplifying each analogue waveform with no complex signal processing such as a pre-equalizing filter to compensate the slope of the frequency response. In this way it is easy to implement actual transmission signal processors. In this experiment, the PEIFoF signal was generated by offline processing.

The PEIFoF signal generated by the AWG was input to the Mach-Zehnder modulator (MZM) that modulated the 1550 nm laser diode (LD) source and then transmitted the result over 11.94 km of single mode fibre (SMF). At the RU side, the PEIFoF signal was detected by the PD and sampled by the 28 Gsps ADC. The sampling data was input to the FPGA on which 3-stage DDC processing was implemented. The DDC processing at each stage has three functions that operate in the time domain, a frequency shifter giving a frequency offset, a half-band filter suppressing the signal in the upper half of the Nyquist zone, and 1/2 decimation reducing the sampling rate to half the input rate. Tab. 1 summarizes the latency of each DDC processor in the FPGA. Each stage had the same latency because the design differs only in the number of parallel calculations. The total latency was 182.4 ns. This value was low enough for the beyond-5G requirement (≤100 us). The 3-stage DDC produces bands #1–4. Each output has a total frequency offset corresponding to the IF offsets of chs #1–4. Then, each of channels #1–4 was demodulated from DDC output bands #1–4 and their error-vector-magnitudes (EVMs) were evaluated to give the quality of the radio signals.

Prior to evaluating the performance of this system, a calibration IFoF signal with flattened pre-emphasis factors 1, α=1, β=1 and γ=1, was transmitted to determine the pre-emphasis factors for improved transmission performance. The calibration IFoF signal had the spectrum shown in Fig. 2. When this calibration signal was transmitted, the amplitude spectrum densities (ASDs) of each channel #1–4 were calculated for each of the DDC output bands #1–4, and the ratios of the ASDs of channels #1–4 were also calculated. To calculate the ASDs of each channel, the fast-Fourier-transform (FFT) powers of each DDC output were summed, and the square root taken. Fig. 3 shows the FFT power spectra of the DDC outputs in the case of calibration IFoF transmission. The ratios of the ASDs were α=1.24, β=2.14 and γ=4.04.

Experimental results

In this section, we explain the experimental results obtained from the experimental setup (Fig. 1) described in the previous section and discuss the performance of the 28 Gsps DDC demultiplexer in the PEIFoF transmission system. In this experiment, the pre-emphasis factors α, β, and γ were the values calculated from the calibration IFoF transmission. Fig. 4 shows the spectrum of the PEIFoF signal. The channels aggregated into higher IFs had higher power than reference channel #1.

Fig. 5 (a)–(d) shows the constellation diagrams of the 3200 symbols demodulated from chs #1–4 modulated by OFDM-16QAM. All channels had clear constellations, and the values of the evaluated root mean square EVM (rmsEVM) for each of chs #1–4 were 8.61%, 8.27%, 7.45% and 8.68%, respectively. In the same way, a PEIFoF signal carrying four OFDM-

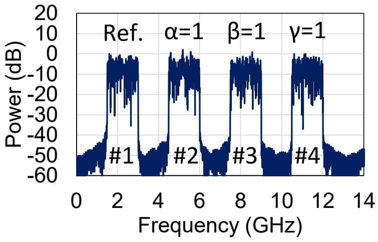

Fig. 2: Calibration IFoF signal spectrum.

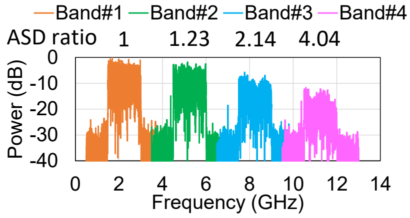

Fig. 3: FFT results from the DDC outputs in the case of calibration IFoF transmission.

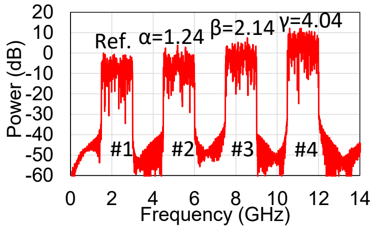

Fig. 4: PEIFoF signal spectrum.

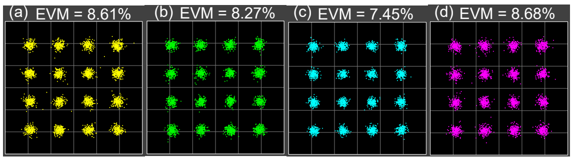

Fig. 5: Constellation diagrams of demultiplexed OFDM-16QAM IF channels (3200 symbols), (a)–(d): channels #1–4.

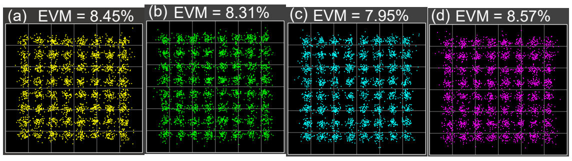

Fig. 6: Constellation diagrams of demultiplexed OFDM-64QAM IF channels (3200 symbols), (a)–(d): channels #1–4.

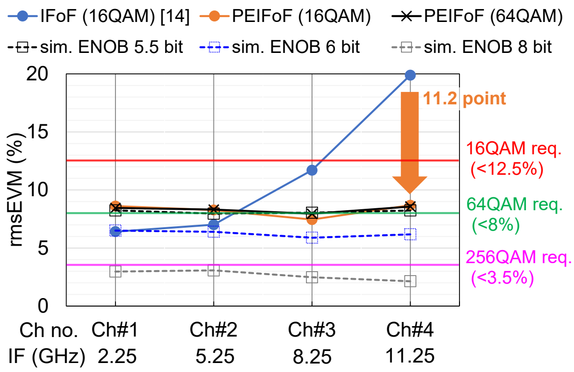

Fig. 7: Evaluated EVMs of each demultiplexed channel transmitted by PEIFoF and IFoF with DDC demultiplexer.

64QAM channels was generated at the DU side in Fig. 1, and the quality of these channels was evaluated. Fig. 6 (a)–(d) shows the constellation diagrams of the demultiplexed OFDM-64QAM. The rmsEVMs of chs #1–4 were 8.45%, 8.31%, 7.95% and 8.57%, respectively. These evaluated values of signal quality are shown in Fig. 7 and compared with the values in the case of IFoF [14]. It is shown that applying in the PEIFoF transmission system investigated in this work, the signal quality from the DDC demultiplexer is improved greatly. In particular, the improvement at the highest frequency channel was 11.2 percentage points, and the average of all channels was 8.3%. In Fig. 7, the red and green solid lines indicate the 3GPP requirements for 16QAM and 64QAM respectively. According to the 3GPP specification, the rmsEVM of a radio signal must be lower than 12.5% for 16QAM and 8% for 64QAM, respectively [15]. The values of rmsEVM in the case of OFDM-16QAM transmission satisfied the 3GPP requirement, so that we obtained adequate transmission performance for 16QAM. On the other hand, in the case of OFDM-64QAM, the rmsEVM of the worst quality channel was only 0.6% short for the requirement. The ENOB of the ADC in the IFoF receiver prototype limited the transmission performance of the demonstration system. In Fig. 7, we added the simulation results in the case of ADC ENOBs of 5.5, 6 and 8 indicated by the black, blue and grey dashed lines respectively. The simulation results indicate that if we got just 0.5 bit improvement of the ENOB, the PEIFoF transmission system with the digital demultiplexer could accommodate OFDM-64QAM radio signals. Furthermore, the realization of an over 20 Gsps class ADC that has an ENOB of 8 would enable even OFDM-256QAM signal transmission, which requires the rmsEVM of <3.5% shown in Fig. 7 by the magenta solid line.

Conclusions and potential future work

We demonstrated four channels 1.5 GHz wideband radio signals transmission for beyond-5G with an FPGA-based receiver and digital pre-emphasis by a simple processing scheme. As a result, the performance satisfied the 3GPP EVM requirement for OFDM-16QAM. We overcame the degradation of the higher frequency response of IFoF transmission and the inadequate ADC ENOB of the digital demultiplexer. In this work, although we used a 28 Gsps ADC whose ENOB was about 5.5, higher bit resolution ADC technology has also steadily matured [16]. Thus, this transmission system can accommodate even higher-order multi-level modulated radio signals such as OFDM-64QAM/256QAM in the near future.

Acknowledgements

This work was in part supported by the commissioned research (No. 20701, No.01401) of National Institute of Information and Communications Technology (NICT), Japan.

References

[1] KDDI Corporation and KDDI Research Inc. "Beyond 5G/6G white paper," ver. 2.0.1, https://www.kddi-research.jp/sites/default/files/kddi_whitepaper_en/pdf/KDDI_B5G6G_WhitePaperEN_2.0.1.pdf, accessed on 13 April 2023.

[2] M. Hörberg, B. Madeberg, D. Sjöberg, H. Zirath, K. Bitsikas, K. Kravariotis, S. Tsapalis, M. Gavell, G. Granström, R. Lövblom, D. Siomos, S. Agneessens, and J. Hansryd, "A W-band, 92-114 GHz, real-time spectral efficient radio link demonstrating 10 Gbps peak rate in field trial," in *Proceedings 2022 IEEE/MTT-S International Microwave Symposium (IMS 2022)*, Denver, Colorado, USA, Aug. 2022, We2G-2, DOI: 10.1109/IMS37962.2022.9865473.

[3] H. Xu, Y. Zhu, Y. Wu, C. Browning, L. Barry, and Y. Yu, "Crosstalk and power fading in a WDM-RoF based MFN using directly modulation 3s-DBR laser," in *Proceedings 2021 Asia Communications and Photonics Conference (ACP)*, Shanghai, China, Oct. 2021, T2H.3.

[4] H. Xu, A. Delmade, C. Browning, A. Atieh, Y. Yu, and L. Barry, "Demonstration of high capacity bidirectional A-RoF system using wavelength reuse and frequency multiplexing," Journal of Lightwave Technology, vol. 41, no. 8, pp. 2343-2350, 2023, DOI: 10.1109/JLT.2022.3230741.

[5] CPRI specification V7.0, http://www.cpri.info/downloads/CPRI_v_7_0_2015-10-09.pdf, accessed on 13 April 2023.

[6] Y. Tong, C. Chow, G. Chen, C. Pen g, C. Yeh, and H. Tsang, "Integrated silicon photonics remote radio frontend (RRF) for single-sideband (SSB) millimeter-wave radio-over-fiber (ROF) systems," *IEEE Photonics Journal*, vol. 11, no. 2, 2019, DOI: 10.1109/JPHOT.2019.2898938.

[7] L. Bogaert, J. Kerrebrouck, H. Li, I. Paula, K. Gasse, C. Wu, P. Ossieur, S. Lemey, H. Rogier, P. Demeester, G. Roelkens, J. Bauwelinck, and G. Torfs, "Siphotonics/GaAs 28-GHz transceiver with reflective EAM for laser-less mmwave-over-fiber," *Journal of Lightwave Technology*, vol. 39, no. 3, 2021, DOI: 10.1109/JLT.2020.3021175.

[8] C. Lim, and A. Nirmalathas, "Radio-over-fiber technology: present and future," *Journal of Lightwave Technology*, vol. 39, no. 4, 2021, DOI: 10.1109/JLT.2020.3024916.

[9] K. Tanaka, S. Ishimura, A. Bekkali, K. Nishimura, and M. Suzuki, "Evolution scenario of optical access infrastructure for supporting beyond-5G mobile systems," in *Proceedings 24th Opto-Electronics and Communications Conference/International Conference on Photonics in Switching and Computing (OECC/PSC)*, Fukuoka, Japan, July 2019, S1-6, DOI: 10.23919/PS.2019.8818057.

[10] S. Ishimura, A. Bekkali, K. Tanaka, K. Nishimura, and M. Suzuki, "Tb/s-class CPRI-equivalent data rate transmission using IF-over-fiber system for high-capacity mobile fronthaul links," in *Proceedings 24th Opto-Electronics and Communications Conference/International Conference on Photonics in Switching and Computing (OECC/PSC)*, Fukuoka, Japan, July 2019, TuA3-1, DOI: 10.23919/PS.2019.8817816.

[11] S. Ishimura, H. Y. Kao, K. Tanaka, K. Nishimura, and M. Suzuki, "IF-over-fiber transmission of 40×400-MHz 256QAM OFDM signals using commercial 100Gb/s EML TOSA for analog mobile fronthaul networks," in *Proceedings 2020 Opto-Electronics and Communications Conference (OECC)*, Taipei, Taiwan, Oct. 2020, T1-2.4, DOI: 10.1109/OECC48412.2020.9273690.

[12] H. Sano, R. Fujihara, S. Nakamura, M. Binkai, F. Shoda, and N. Ohata, "A high capacity and cost-effective OFDM EML TO-CAN for RoF/IFoF transmission systems in beyond-5G mobile fronthaul," in *10th IEEE CPMT Symposium Japan (ICSJ)*, Kyoto, Japan, Nov. 2021, Paper 62, DOI: 10.1109/ICSJ52620.2021.9648882.

[13] H. Y. Kao, S. Ishimura, K. Tanaka, K. Nishimura, and R. Inohara, "End-to-end demonstration of fiber-wireless fronthaul networks using a hybrid multi-IF-over-fiber and radio-over-fiber system," *IEEE Photonics Journal*, vol. 13, no. 4, Aug. 2021, DOI: 10.1109/JPHOT.2021.3106706.

[14] J. Nishioka, T. Akamatsu, T. Yoshida, Y. Konishi, M. Hayama, K. Onohara and N. Suzuki, "Digital-down-conversion of OFDM-QPSK/16QAM signals at 28 Gsps for beyond-5G intermediate frequency over fiber," in *Proceedings 27th Opto-Electronics and Communications Conference/International Conference on Photonics in Switching and Computing (OECC/PSC)*, Toyama, Japan, July 2022, MF1-2, DOI: 10.23919/OECC/PSC53152.2022.9850024.

[15] 3GPP TS 38.521-1 ver. 16.6.0 release 16, https://www.etsi.org/deliver/etsi_ts/138500_138599/13852101/16.06.00_60/ts_13852101v160600p.pdf, accessed on 13 April 2023.

[16] B. Murmann, "ADC performance survey 1997-2022," http://web.stanford.edu/~murmann/adcsurvey.html, accessed on 13 April 2023.